Electronic absorption spectroscopy of matrix-isolated polycyclic aromatic hydrocarbon cations. II. The phenanthrene cation ($C_{14}H_{10}^+$) and its 1-methyl derivative

F. Salama, C. Joblin, and L. J. Allamandola
NASA-Ames Research Center, Space Science Division, Moffett Field, California 94035-1000

(Received 15 August 1994; accepted 12 September 1994)

The ultraviolet, visible, and near infrared absorption spectra of phenanthrene ($C_{14}H_{10}$), 1-methylphenanthrene [$(CH_3)C_{14}H_9$], and their radical ions [$C_{14}H_{10}^+$; $(CH_3)C_{14}H_9^+$], formed by vacuum-ultraviolet irradiation, were measured in neon matrices at 4.2 K. The associated vibronic band systems and their spectroscopic assignments are discussed. The oscillator strengths were calculated for the phenanthrene ion and found lower than the theoretical predictions. This study presents the first spectroscopic data for phenanthrene and its methyl derivative trapped in a neon matrix where the perturbation of the isolated species by its environment is minimum; a condition crucial to astrophysical applications. © *1994 American Institute of Physics.*

I. INTRODUCTION

The recognition of the potential importance of polycyclic aromatic hydrocarbon (PAHs) in astrophysics[1] has motivated our study of the ultraviolet, visible, and near-infrared spectroscopic characteristics of these molecules in their neutral and ionized forms. PAHs are currently considered the best candidates to explain the mid-infrared spectral features (UIR bands) at 3.3, 6.2, 7.7, 8.6, and 11.3 μm emitted from many objects in the interstellar medium.[2] PAHs have also been proposed as possible carriers of the visible, diffuse interstellar absorption bands (DIBs)[3(a)–3(c)] which extend from 4000 Å into the near IR and are characteristic of an important, ubiquitous component of interstellar space.[3(d)–3(f)] Both hypotheses require interstellar PAHs to be present as a mixture of radicals and ions as well as neutral species (perhaps partially hydrogenated and/or containing side groups). In the first part of this program, small PAHs, i.e., molecules with less than 25 carbon atoms, have been considered. Experimental results, as well as their astrophysical implications, have been previously reported and discussed for the electronic transitions of the naphthalene ($C_{10}H_8^+$),[4] pyrene ($C_{16}H_{10}^+$),[5] and 1-pyrenecarboxaldehyde [$(COH)C_{16}H_9^+$] (Ref. 6) cations isolated in argon and neon matrices. A theoretical study of the electronic spectra of the hydrogen abstraction and addition derivatives of naphthalene ($C_{10}H_7$ and $C_{10}H_9$) in their neutral, anionic, and cationic states has also been performed.[7] Here, we report the experimental results for the phenanthrene molecular ion ($C_{14}H_{10}^+$) and its derivative 1-methylphenanthrene [$(CH_3)C_{14}H_9^+$] isolated in neon matrices. It is the purpose of these studies to obtain quantitative ultraviolet-visible-near-infrared spectroscopic data on isolated, neutral, and ionized PAHs.

Matrix isolation spectroscopy[8] is a particularly well suited technique for the simulation of an astrophysical environment in the case of large, reactive species such as ionized PAHs. It permits the simulation of low temperature (4–15 K) and isolated conditions in space. Among the rare gases commonly used as matrix-cage material (Ne, Ar, Kr, and Xe), solid neon provides the best (i.e., less polarizable) medium for the study of quasiunperturbed electronic spectra of ions.[9]

The phenanthrene cation has been studied in detail in the ultraviolet-to-near-infrared range by absorption spectroscopy in glassy organic and inorganic solids,[10] in solution,[11] and in argon matrices.[6,12] Gas-phase data have been provided by the photoelectron spectra (PES) of phenanthrene.[12(b),13] Recently, higher resolution photoelectron spectroscopy coupled to resonance enhanced multiphoton ionization (REMPI), has provided information on the vibrational levels of the ion ground electronic state.[13(d)] Phenanthrene and 1-methylphenanthrene cations were formed, here, by direct photoionization of the matrix-isolated neutral precursors [$C_{14}H_{10}$ and $(CH_3)C_{14}H_9$] and the vibronic absorption spectra were recorded from 200 nm (50 000 cm^{-1}) to 1050 nm (9500 cm^{-1}).

The ultraviolet-visible-to-near infrared spectrograph coupled with a low temperature (4.2 K) sample chamber is briefly described in Sec. II. The following section, III, presents the absorption spectra of neutral phenanthrene and 1-methylphenanthrene and their cations. The discussion of the results and the spectroscopic assignments are reported in Sec. IV, and the conclusions of the study are given in the last section (V).

II. EXPERIMENT

A UV-visible-to-near infrared spectrograph, coupled to a helium-cooled cryogenic cell, is used to measure the absorption spectra of neutral and ionic PAHs using matrix isolation spectroscopy. The experimental apparatus has been described in detail in a previous report[4(a)] and only a brief review, focusing on the characteristics of the new detection system, is given here. The apparatus consists of the following parts:

(a) The spectral light source (LS). A deuterium lamp (Hamamatsu L 1626) provides a smooth continuum from 160 to 360 nm and a quartz tungsten halogen lamp (Ushio FCR) provides a stable output from 320 to 2500 nm.

(b) The cryogenic sample chamber (SC). The sample chamber is equipped with four ports at 90° and two gas injection ports at 45° angles. The cryogenic sample

 0021-9606/94/101(12)/10252/11/$6.00

holder, suspended in the center of the chamber at the tip of the cooler, holds a sapphire window (S). A high vacuum (P in the order of 10^{-8} T) is maintained while the substrate is cooled down to 4.2 K by an extended liquid helium transfer cryostat (Hansen Associates HLT-183). The temperature of the substrate is controlled by regulating the liquid helium flow. The temperature of the substrate is measured with an Fe–Au/Chromel thermocouple connected to the sample holder. The substrate can be positioned to face alternatively the spectroscopy ports, the gas injection ports, an excitation lamp, or a vacuum deposition furnace.

(c) The monochromator (M). A triple grating monochromator (Acton Research Corporation SpectraPro-500) with an effective focal length of 568.2 mm and an aperture ratio f/6.9 is used. Ruled gratings (1200, 600, and 300 grooves/mm) blazed at 300 and 650 nm are used. The nominal linear dispersion is 1.7, 3.4, and 6.8 nm/mm, respectively, over the entire wavelength range (180–1050 nm) for these three gratings. The entrance slit is adjustable with a micrometer (0.01 μm–3.0 mm range). An external scan controller interfaced to the serial port (RS-232) of a computer system (Microlink Data Systems) is used to remotely drive the monochromator. An UV fiber optic cable guides the focused light collected at the spectroscopy port of the cryogenic sample chamber to an optical fiber adaptor (OFA) mounted on the entrance slit. The exit port is equipped with a CCD detector mounting flange.

(d) The photon detector (CCD). The detector is a thermoelectrically cooled charge coupled device (CCD) area array detector (Princeton Instruments, model TE/CCD-1152) with a 298 (column) by 1152 (row) pixel format. The active area is 6.7×26.0 mm with a pixel size of 22.5×22.5 μm. The CCD, operated at −40 °C with tap water circulation, is coated with a UV-to-visible converter making it sensitive in the spectral range 180–1060 nm (peaking near 750 nm). The CCD is mounted directly on the exit port of the monochromator and interfaced to an IBM clone computer through a 16 bit A/D controller (Princeton Instruments, model ST-130).

(e) The photoexcitation source (ES). Vacuum ultraviolet radiation is generated by a microwave-powered, hydrogen flow, discharge lamp (Opthos Instruments) equipped with a removable MgF_2 window and mounted on one of the ports of the sample chamber. When operating with pure H_2 at a pressure of 1–2 T, the flux is $\sim 2\times10^{15}$ photons cm^{-2} s^{-1} equally distributed between the 160 nm band and the Lyman α line at 121.6 nm (10.2 eV). By using a 10% hydrogen/helium mixture in a low pressure discharge one can get most of this flux as nearly monochromatic radiation in the Lyman α line.

The entire system is monitored and controlled with a computer system (Microlink Data Systems, type 486DX/33).

III. RESULTS

Each experiment consisted of the following protocol: recording of the single-beam absorption spectrum of the cold blank substrate (I_{blank}), simultaneous condensation of the sample with the argon/neon matrix gas on the cold window at 4.2 K, measurement of the single-beam absorption spectrum of the matrix-isolated neutral precursor ($I_{neutral}$), exposure of the sample to VUV irradiation for a given time, t, and, finally, recording of the single-beam absorption spectrum of the irradiated sample (I_{irrad}). The last two steps were repeated at different intervals to monitor the dependence of the new spectral features produced on VUV photolysis. The ion yield was optimized by setting the different parameters such as duration of VUV irradiation, concentration of phenanthrene in the rare gas matrix, photon energy of the excitation source in the VUV (i.e., the flux of the hydrogen Lyman α line with respect to the 160 nm band), and *in situ* photolysis to the values determined in our previous studies.[4(a),4(b)] In some cases, 2 or 3 layers of irradiated sample were formed on top of each other to increase the ion column density. All spectra were recorded over the entire range of the spectrophotometer system (180–1050 nm) at a nominal resolution of 0.1 nm. Samples were prepared by codepositing phenanthrene (or 1-methylphenanthrene) vapor with the rare gas (Ar or Ne) at room temperature. The phenanthrene and 1-methylphenanthrene gases were deposited through a tube at 45° with respect to the rare gas deposition line. Phenanthrene and 1-methylphenanthrene have low vapor pressures of about 14 and 3 mT, respectively, when in equilibrium with the solid at room temperature.[14] This is sufficient, however, for the preparation of rare gas matrix samples. The spectroscopic results described in this section were generally obtained under the following standard experimental conditions (unless specified otherwise): R ($C_{14}H_{10}$): M (Ne)=1: 1000; substrate temperature, 4.2 K; sample deposition rate, 10 mmol h^{-1}; monochromatic VUV irradiation in the Lyman α line (10.2 eV). Phenanthrene crystals (Aldrich 99.5%), Ar (Matheson 99.9995%), and Ne (Cryogenic Rare Gas 99.999%) research grade rare gases were used without further purification.

A. Neutral phenanthrene

The absorption spectrum of Phenanthrene isolated in an Ar or Ne matrix can be divided into nine distinct band systems across the wavelength range 200–1050 nm.[15] Eight band systems, all associated with the singlet manifold, are measured in the 200–340 nm region (see Fig. 1). The longest wavelength system, or system I, is very weak, with an oscillator strength, f, of 0.0002.[15] The strongest band of this system falls at 341.1±0.1 nm in Ne and 343.3±0.2 nm in Ar. System II peaks at 284.3±0.1 nm in Ne (289.7±0.2 nm in Ar) and is moderately strong (f=0.0766).[15] Systems III and IV are weak and peak at 273.4±0.1 nm (f=0.0168) (Ref. 15) and 262.4±0.1 nm (f=0.0132),[15] respectively. System V is very strong (f=1.1874) (Ref. 15) with the strongest band at 243.0±0.1 nm in Ne and 246.8±0.1 nm in Ar. System VI is moderately strong (f=0.0885) (Ref. 15) with the strongest band at 229.0±0.3 nm. Systems VII is moderately strong (f=0.3155) (Ref. 15) and peaks at 214.5±0.3 nm in Ne and 216.7±0.2 nm in Ar. Finally, system VIII peaks at 204.5 nm±0.3 nm in Ne with f=0.061. A very weak absorption, associated to the triplet manifold,[15] is measured at 363.7

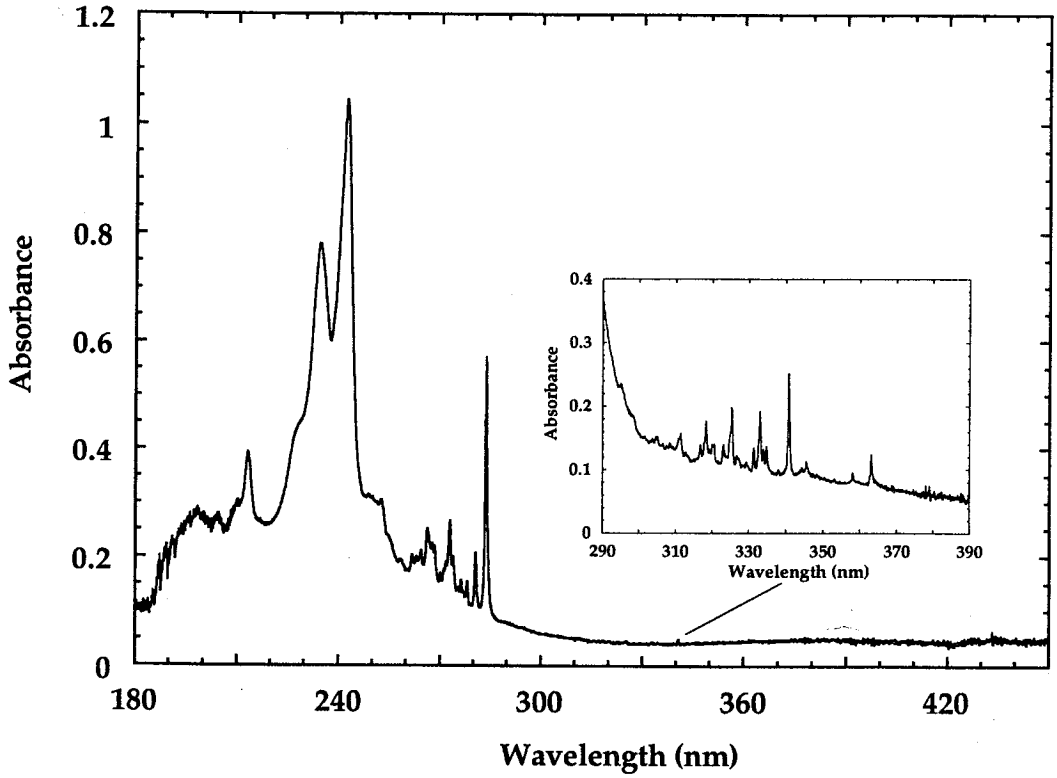

FIG. 1. The absorption spectrum of phenanthrene isolated in a neon matrix ($M/R=1000$, deposition rate=10 mmol h^{-1}, $T=4.2$ K). Full spectrum corresponds to 2 min deposition. Insert corresponds to 35 min deposition.

± 0.1 nm in Ne. The vibronic band wavelengths, frequencies, and intervals are listed in Table I for a Ne matrix. The vibronic spacings listed are broken down into possible fundamental modes. These fundamentals and their assignments are summarized in Table III where they are compared to the experimental and theoretical spectroscopic data available in the literature[16,19(a)] (see Sec. IV A). The data indicate a red shift in energy for all the levels when going from a neon to an argon matrix as expected from the fourfold increase in the polarizability of the matrix material.[17] The wide range in oscillator strengths of these systems required distinct matrix thicknesses to optimize the spectrum of each particular system

B. Neutral 1-methylphenanthrene

The absorption spectrum of 1-methylphenanthrene isolated in a Ne matrix resembles that of phenanthrene. It too can be divided into distinct band systems, with very different intensities, in the 200–1050 nm wavelength range (Fig. 2). By analogy with phenanthrene (Sec. III A), we have tentatively divided the observed absorption bands into 7 band systems (6 systems belonging to the singlet manifold and 1 system belonging to the triplet manifold). The longest wavelength system of the singlet manifold, or system I, is very weak, with the strongest band falling at 343.8 ± 0.1 nm. Systems II and III are moderately strong and peak at 290.5 ± 0.1 and 269.3 ± 0.1 nm, respectively. Only one band of system IV is observed at 255.2 ± 0.1 nm. System V is very strong with the stronger bands at 246.3 ± 0.1 nm and 238.8 ± 0.1 nm. The weak system VI is not observed. System VII is the shortest wavelength system observed with the strongest band at 216.6 ± 0.1 nm. A very weak absorption, associated with the triplet manifold by analogy with phenanthrene (Sec. III A), is measured at 366.1 ± 0.1 nm. The vibronic band wavelengths, frequencies and intervals are listed in Table II. The vibronic spacings listed are broken down into possible fundamental modes. These fundamentals and their assignments are summarized in Table III where they are compared to the experimental and theoretical spectroscopic data available for phenanthrene in the literature[16,19(a)] (see Sec. IV A). The data indicate a red shift in energy for all the transitions when going from phenanthrene to its 1-methyl derivative as expected from an increase in the polarizability of the species containing a side group. [A similar effect has been observed for 4-methylphenanthrene in solution at room temperature[21] and in Shpolskii matrices at 77 K.[20] For example, the *same* red shift of 230 cm^{-1} is measured for the $S_1 \leftarrow S_0$ transition peak when going from phenanthrene to 4-methylphenanthrene in Shpolskii matrices at 77 K (Ref. 20) and from phenanthrene to 1-methylphenanthrene in neon matrices at 4.2 K (compare Tables I and II).] The relative shift $[\Delta\nu_{(\text{Phenanthrene-Methylphenanthrene})}/\nu_{\text{phenanthrene}}]$, reported in Table II, is proportional to the energy of the transition and increases from 0.6% for the triplet system, to a value of about 1%–2% for the systems belonging to the singlet manifold. This would tend to indicate that the interaction between the

TABLE I. Vibronic transitions of neutral phenanthrene isolated in a neon matrix. (Electronic transitions assigned following Ref. 15.)

λ (nm)	ν (cm^{-1})	$\Delta\nu$ (cm^{-1})
Singlet system VIII: 4 $^1B_2(S_8)\leftarrow X\ ^1A_1(S_0)$		
204.5[a]	48 900	...
Singlet system VII: 5 $^1A_1(S_7)\leftarrow X\ ^1A_1(S_0)$		
211.5[a]	47 281	661
214.5 (0.20)[b]	46 620	0
Singlet system VI: 4 $^1A_1(S_6)\leftarrow X\ ^1A_1(S_0)$		
229.0 (sh)	43 668	...
Singlet system V: 3 $^1B_2(S_5)\leftarrow X\ ^1A_1(S_0)$		
235.2 (0.05)	42 517	1365
243.0 (0.10)[b]	41 152	0
Singlet system IV: 3 $^1A_1(S_4)\leftarrow X\ ^1A_1(S_0)$		
250.0 (sh)	40 000	1890 (1369+500)
253.3 (0.10)	39 479	1369
259.0 (0.15)	38 610	500
262.4 (0.05)[b]	38 110	0
Singlet system III: 2 $^1B_2(S_3)\leftarrow X\ ^1A_1(S_0)$		
263.5 (0.05)	37 951	1375
265.0 (0.05)	37 736	1160
267.2 (0.10)	37 425	849
268.2 (0.10)	37 286	710
273.4 (0.05)[b]	36 576	0
Singlet system II: 1 $^1B_2(S_2)\leftarrow X\ ^1A_1(S_0)$		
274.4 (sh)	36 443	1269
276.9 (0.05)	36 114	940
278.7 (0.05)	35 881	707
281.2 (0.05)	35 562	388
284.3 (0.04)[b]	35 174	0
Singlet system I: 2 $^1A_1(S_1)\leftarrow X\ ^1A_1(S_0)$		
311.7 (0.12)	32 082	2765 (2×1386)
317.2[a]	31 526	2209 (1386+822)
318.7 (0.05)	31 378	2061 (1386+677)
320.4[a]	31 215	1898 (1386+516)
323.4[a]	30 922	1605
325.3 (0.05)	30 741	1424
325.7 (0.05)	30 703	1386
331.8 (0.05)	30 139	822
333.4 (0.05)	29 994	677
334.4 (0.05)	29 900	583
335.2 (0.05)	29 833	516
338.4[a]	29 551	234
341.1 (0.10)[b]	29 317	0
Triplet system I: 1 $^3A_1(T_2)\leftarrow X\ ^1A_1(S_0)$		
346.1[a]	28 893	1398
358.9[a]	27 863	368
363.7 (0.10)[b]	27 495	0

[a]Represents a single measurement with a 0.5 nm uncertainty; sh, band shoulder.

[b]Strongest band of the system. The number in parentheses indicates the value of σ^2.

1-methylphenanthrene molecule and the rare gas atoms of the lattice increases as higher excited molecular electronic states are reached. The wide range in oscillator strengths of these systems required distinct matrix thicknesses to optimize the spectrum of each particular system.

C. Phenanthrene cation

VUV irradiation of the sample (10.2 eV) produces new spectral features in the 300–910 nm range [Figs. 3 and 5(a)]. Six new band systems are detected. The new absorption bands, together with their assignments, frequencies and frequency intervals, are summarized in Table IV. The strongest peak in the longest wavelength system measured falls at 898.3±0.1 nm [80 cm^{-1} full-width at half-maximum (FWHM)]. This band dominates the entire spectrum in the visible-NIR range (i.e., 400–1050 nm). A very weak absorption (not shown) is measured at 634.4±0.5 nm. Three other systems peak at 470.7±0.2, 425.8±0.3, and 396.0±0.3 nm, respectively. The highest energy system, which peaks at 344.9±0.5 nm (not shown), falls in a region obscured by neutral phenanthrene. The associated band, although difficult to measure, seems to be correlated with the visible bands. [In some cases, the sample was formed using lower deposition rates (Ne flow=5 mmol h^{-1}, phenanthrene crystals maintained at 10 °C). In such cases, we have observed a constant splitting of the order of 20 cm^{-1} for all the spectral features in the 600–1040 nm range while the shorter wavelength bands appeared unaffected. The three longest wavelength pair of bands fall at (898.5 and 896.7 nm; 66 cm^{-1} total FWHM), (879.5 and 877.8 nm) and (856.9 and 855.5 nm). This effect can be interpreted in terms of crystal-field splitting[9(b)] due to the increasing degree of crystallinity of the matrix in contrast to the general case where an amorphous matrix is formed.]

We attribute all of these new features produced by VUV irradiation to the phenanthrene cation ($C_{14}H_{10}^+$) on the basis of their similarities in position, relative intensities, and general behavior under irradiation to those previously assigned to this ion and measured with different cation formation techniques.[10–13] The strong absorption band measured at 898.3 nm in neon is close—within the expected matrix-induced shift (see below)—to the 899.8 nm band position measured for Ar-matrix isolated $C_{14}H_{10}^+$ formed by photoionization of neutral phenanthrene $C_{14}H_{10}$ at 20 K.[12] Good agreement is also found with the peak position of $C_{14}H_{10}^+$ in γ-irradiated glasses at 77 K—915 nm in organic matrices[10(b)] and 913 nm in a Freon glass[10(b)]—and in UV-irradiated boric acid glasses at room temperature (893 nm).[10(c)] Similar agreement is found when comparing the other band system origins listed in Table IV with the values of 485, 428, and 403 nm in Freon glasses,[10(b)] 500, 430, 403, and 356 nm in organic matrices,[10(b)] 606, 476, 427, 402, and 338 nm in boric acid glasses,[10(c)] and 641, 473.7, 431, 398, and 346 nm in Ar matrices.[6,12] The data indicate a red shift in energy for all the transitions of $C_{14}H_{10}^+$ when going from a neon to an argon matrix. The Ne-to-Ar relative shifts in the energy of the vibronic levels ($\Delta\nu/\nu_{Ne}$) increase from a mean value of about 0.15% for the NIR system (898.3 nm in Ne) to 0.3% for the NUV system (344.9 nm in Ne).

Our results also show a very good correlation with the measured photoelectron spectra (PES) of gas phase phenanthrene.[12(b),13(a),13(b),13(c)] The comparison between the gas phase PES band differences [$(I_n - I_1)$, where I_n is the nth ionization potential with $n>1$] and our Ne matrix absorption measurements, reported in Table V, shows that the

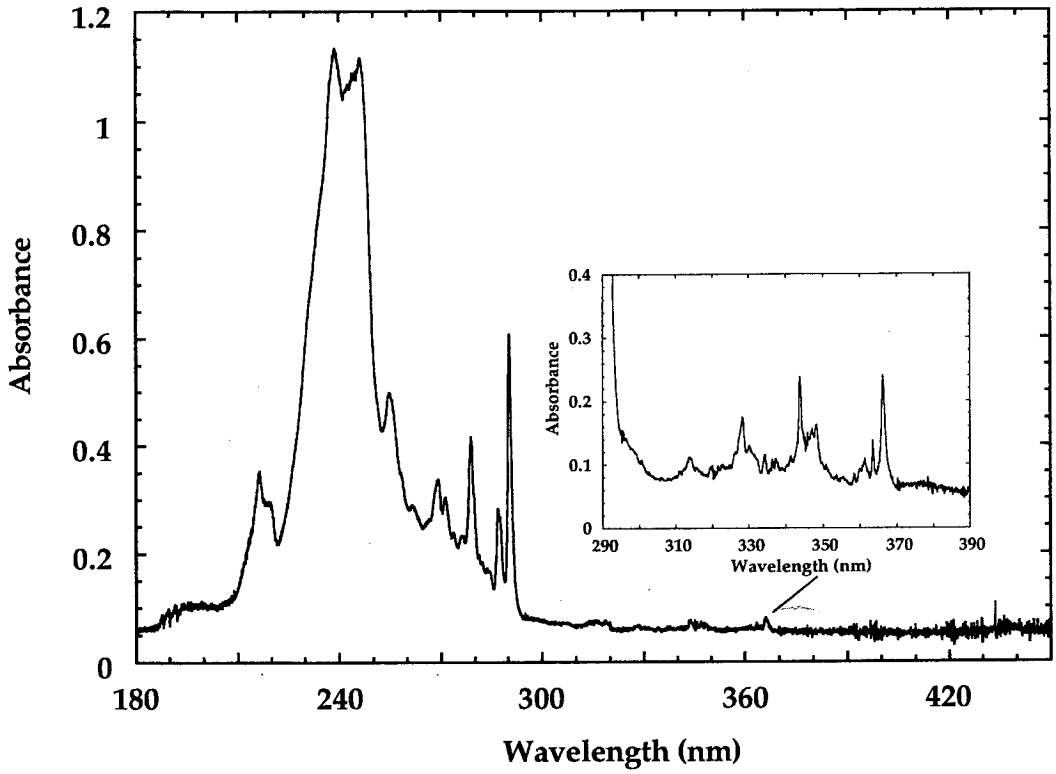

FIG. 2. The absorption spectrum of 1-methylphenanthrene isolated in a neon matrix ($M/R=1000$, deposition rate=10 mmol h^{-1}, $T=4.2$ K). Full spectrum corresponds to 18 min deposition. Insert corresponds to 165 min deposition.

reported difference in energy between the first and third PES peaks (I_3-I_1) is in extremely good agreement with the matrix measurements of 11 132±2 cm^{-1} (898.3 nm) in Ne for the corresponding absorption system origin. Similarly, the other weaker visible absorption progressions associated with $C_{14}H_{10}^+$ and observed at 15 763±10 cm^{-1} (634.4 nm) and 21 245±10 cm^{-1} (470.7 nm) in a Ne matrix are very close to the reported (I_4-I_1) and (I_5-I_1) energy differences of the PES data. No further correspondence can be established between the optical and PES spectral features of $C_{14}H_{10}^+$ since the latter measurements can only be compared with the photon-induced absorptions corresponding to transitions from the fully occupied molecular orbitals and the partially occupied orbital of the π bonding system. PES peak assignments are also given in Table V.

Finally, various types of open-shell SCF-CI calculation methods[12(b),10(c)] predict *only seven* optically allowed electronic transitions of the phenanthrene cation in the 300–1050 nm range and verify the attribution of the six band systems to the phenanthrene cation as listed in Table IV. [Note: The lowest energy band system of $C_{14}H_{10}^+$, falls in the infrared, at about 4.3 μm,[13] and cannot be measured with our current set up (the detector response cutoff is 1060 nm)].

D. 1-methylphenanthrene cation

VUV irradiation of the sample (10.2 eV) produces new spectral features in the 300–950 nm range [see Figs. 4 and 5(b)]. The spectrum of the 1-methylphenanthrene cation is very similar, in its appearance, to that of the phenanthrene cation (compare Figs. 3 and 4). Five new band systems are detected. The new absorption bands, together with their frequencies and frequency intervals, are summarized in Table IV where they are compared to the corresponding transitions of the phenanthrene cation. All the transitions are red shifted in energy when going from the phenanthrene cation to its 1-methyl derivative as expected from an increase in the polarizability of the species containing the methyl side group. [The same effect is observed when comparing the spectra of the naphthalene cation $C_{10}H_8^+$ and its 1-methyl derivative $(CH_3C_{10}H_7^+)$.[10(b),18]] The energy shifts [$\Delta\nu_{(\text{Phenanthrene-Methylphenanthrene})}$] measured in neon matrices for each of the cation band systems have mean values of about 365, 320, 820, 600, and 665 cm^{-1}, respectively, when going from the lowest energy to the highest energy transitions (see Table IV). These values translate into relative shifts [$\Delta\nu_{(\text{Phenanthrene-Methylphenanthrene})}/\nu_{\text{phenanthrene}}$] of 3.6%, 1.5%, 3.5%, 2.4%, and 2.3%, respectively, implying a slightly stronger effect of the methyl side group on the low energy transitions of $(CH_3)C_{14}H_9^+$. The strongest peak in the longest wavelength system measured falls at 931.0±0.1 nm (85 cm^{-1} FWHM). This band dominates the entire spectrum in the visible-NIR range (i.e., 400–1050 nm). Three other weaker systems peak at 467.1±0.1, 440.7±0.3, and 404.5 ±0.5 nm, respectively. The highest energy system falls in a region obscured by the neutral precursor. The associated

TABLE II. Vibronic transitions of neutral 1-methylphenanthrene isolated in a neon matrix.

λ (nm)	ν (cm^{-1})	$\Delta\nu$ (cm^{-1})	$\Delta\nu_{Rel}$ (cm^{-1})[a]
System VII: $S_7 \leftarrow S_0$			
216.6 (0.10)[b]	46 168	568	
219.3 (sh)	45 600	0	2.2
System V: $S_5 \leftarrow S_0$			
238.8 (0.05)[b]	41 876	1276	1.5
242.7 (0.20)	41 203	603	
244.0 (sh)	40 984	384	
246.3 (0.05)	40 600	0	1.3
System IV: $S_4 \leftarrow S_0$			
255.2 (0.05)	39 185	0	0.8
System III: $S_3 \leftarrow S_0$			
261.8 (0.1)	38 197	2355 (1291+1018)	
269.3 (0.05)	37 133	1291	
271.3 (0.05)	36 860	1018 (2×509)	
273.8 (0.1)	36 523	681	
279.0 (0.05)[b]	35 842	0	2.0
System II: $S_2 \leftarrow S_0$			
287.2 (0.05)	34 819	396	
290.5 (0.05)[b]	34 423	0	2.1
System I: $S_1 \leftarrow S_0$			
313.6[c]	31 888	2801 (1354+1447)	
315.8 (0.1)	31 666	2579 (1354+1212)	
319.0[c]	31 348	2261 (1354+907)	
328.5 (0.05)	30 441	1354	
330.1[c]	30 299	1212	
343.8 (0.05)[b]	29 087	0	0.8
$T_2 \leftarrow S_0$			
347.8 (0.2)	28 752	1234	
361.3[c]	27 678	363	
363.4[c]	27 518	203	
366.1 (0.05)[b]	27 315	0	0.6

[a]The relative shift is defined as $\Delta\nu_{Rel}$ (cm^{-1}) $=[\Delta(\nu_{Phenanthrene-Methylphenanthrene})/\nu_{phenanthrene}]$.
[b]Strongest band of the system. The number in parentheses indicates the value of σ^2.
[c]Represents a single measurement with a 0.5 nm uncertainty; sh, band shoulder.

TABLE III. Comparison of the repeating vibrational frequencies (in cm^{-1}) for matrix-isolated neutral phenanthrene and 1-methylphenanthrene in their singlet and triplet electronic excited states with the calculated data for phenanthrene in the fundamental electronic state and the supersonic free jet data measured for phenanthrene in the S_1 and S_2 electronic excited states.

Vibrational mode[a]	$C_{14}H_{10}$ theor.[a]	$C_{14}H_{10}$ gas[b]	$C_{14}H_{10}$ Ne[c]	CH_3–$C_{14}H_9$ Ne[c]
A_1 (in-plane)	192			203 (T_2)
B_1 (out-of-plane)	239	236 (S_1)	234 (S_1)	
B_1 (out-of-plane)	403	371 (S_2)	368 (T_2)	363 (T_2)
B_2 (in-plane)	404		388 (S_2)	396 (S_2)
				384 (S_5)
A_1 (in-plane)	511	516 (S_1)	516 (S_1)	509 (S_3)
B_1 (out-of-plane)	499	529 (S_2)	500 (S_4)	
A_2 (out-of-plane)	573	585 (S_1)	583 (S_1)	603 (S_5)
				568 (S_7)
A_1 (in-plane)	675	673 (S_1)	677 (S_1)	681 (S_3)
		675 (S_2)	661 (S_7)	
B_2 (in-plane)	707	704 (S_1)	707 (S_2)	
		717 (S_2)	710 (S_3)	
B_2 (in-plane)	825	824 (S_1)	822 (S_1)	
		824 (S_2)		
B_1 (out-of-plane)	842		849 (S_3)	
B_2 (in-plane)	896	921 (S_2)		907 (S_1)
A_2 (out-of-plane)	953		940 (S_2)	
B_1 (out-of-plane)	957			
A_1 (in-plane)	1156	1158 (S_1)	1160 (S_3)	
		1157 (S_2)		
B_2 (in-plane)	1181			1212 (S_1)
B_2 (in-plane)	1285	1260 (S_2)	1269 (S_2)	1291 (S_3)
				1276 (S_5)
A_1 (in-plane)	1312	1301 (S_2)		
A_1 (in-plane)	1375[d]	1377 (S_1)	1386 (S_1)	1354 (S_1)
B_2 (in-plane)	1373[d]	1388 (S_2)	1375 (S_3)	
			1369 (S_4)	
			1365 (S_5)	
			1398 (T_2)	
A_1 (in-plane)	1431	1430 (S_1)	1424 (S_1)	
B_2 (in-plane)	1432	1430 (S_2)		
B_2 (in-plane)	1450			1447 (S_1)
B_2 (in-plane)	1595	1602 (S_1)	1605 (S_1)	
A_1 (in-plane)	1597	1602 (S_2)		

[a]Reference 16. The symmetry indicated for each vibration is related to the molecular configuration defined in the text.
[b]Reference 19(a).
[c]Ne matrix; this work.
[d]Reference 20(b).

band, although difficult to measure, seems to be correlated with the visible bands and peaks at 353.0±0.1 nm.

We attribute all of these new features produced by VUV irradiation to the 1-methylphenanthrene cation [$(CH_3)C_{14}H_9^+$] on the basis of their similarities in position (taking into account the shift in energy induced by the methyl side group), *relative intensities, and general behavior under irradiation to those previously assigned to the phenanthrene ion* (see Sec. III C). This is, to the best of our knowledge, the first report of the electronic spectrum of the 1-methylphenanthrene cation [$(CH_3)C_{14}H_9^+$].

IV. DISCUSSION AND SPECTROSCOPIC ASSIGNMENTS

A. Neutral phenanthrene

The absorption spectrum of neutral phenanthrene has been studied extensively in the ultraviolet and visible regions of the optical spectrum and the spectroscopy of this molecule is well documented for the gas,[19(a)], liquid,[19(b)] and solid[20] phases. This is, to the best of our knowledge, the first report of the ultraviolet to near-infrared absorption spectrum of phenanthrene embedded in a rare gas (neon) matrix.

Phenanthrene ($C_{14}H_{10}$) is a catacondensed polycyclic aromatic hydrocarbon which belongs to the C_{2v} symmetry group. Phenanthrene has 14 π electrons which produce the low energy singlet–singlet and singlet–triplet transitions (type π–π^*) in the ultraviolet. Figure 1 shows the transitions from the ground (S_0) to the excited singlet states S_i ($i=1$–7) and to one of the excited triplet states (T_2). In this paper, we have chosen the configuration shown in Fig. 6 for the labeling of the molecular axes. The x axis is perpendicular to the plane of the molecule, the y axis corresponds to the long axis

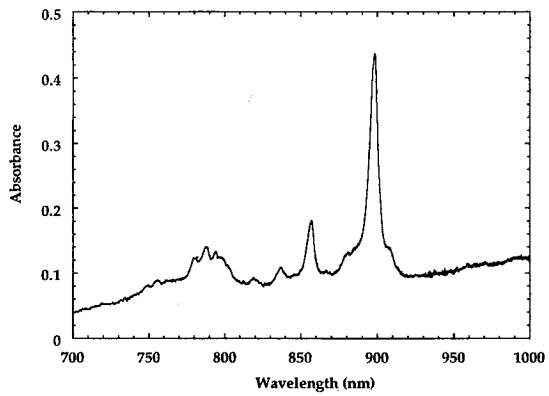

FIG. 3. The $^2A_2(D_2)\leftarrow X\ ^2B_1(D_0)$ transition of the phenanthrene cation isolated in a neon matrix (phenanthrene/neon=1000, deposition rate=10 mmol h^{-1}, T=4.2 K). The spectrum corresponds to six, consecutive, 35 min deposits, each exposed to VUV irradiation for 16 min.

of the molecule, and the z axis is associated with the short axis of the molecule.

According to this convention, and following the assignment of the transitions occurring in phenanthrene,[15] we assign the lowest energy absorption vibronic system (Table I), to the singlet–triplet electronic transition: $1\ ^3A_1(T_2)\leftarrow X\ ^1A_1(S_0)$. All the other, higher energy transitions, are associated with the singlet manifold, and are assigned to the following transitions in order of increasing energy: $2\ ^1A_1(S_1)\leftarrow X\ ^1A_1(S_0)$, $1\ ^1B_2(S_2)\leftarrow X\ ^1A_1(S_0)$, $2\ ^1B_2(S_3)\leftarrow X\ ^1A_1(S_0)$, $3\ ^1A_1(S_4)\leftarrow X\ ^1A_1(S_0)$, $3\ ^1B_2(S_5)\leftarrow X\ ^1A_1(S_0)$, $4\ ^1A_1(S_6)\leftarrow X\ ^1A_1(S_0)$, and $5\ ^1A_1(S_7)\leftarrow X\ ^1A_1(S_0)$. [The $2\ ^1A_1(S_1)\leftarrow X\ ^1A_1(S_0)$ and $1\ ^1B_2(S_2)\leftarrow X\ ^1A_1(S_0)$, transitions correspond to the α and para bands in Clar's notation. In a similar manner, the $3\ ^1B_2(S_5)\leftarrow X\ ^1A_1(S_0)$ and $5\ ^1A_1(S_7)\leftarrow X\ ^1A_1(S_0)$ transitions are associated with the β and β' bands.]

A repeating pattern can be recognized in the energy intervals reported in Table I which, when compared to the experimental and theoretical spectroscopic data available in the literature,[16] allows one to make tentative vibrational assignments. These assignments are listed in Table III for each absorption system in the neon matrix. Moreover, the similarities—within the accuracy of the measurements—in the vibrational frequencies of the modes in the various excited singlet states indicate that the geometry of the molecule is only slightly modified in these different electronic states with respect to that of the ground electronic state. Note also the excellent agreement observed when comparing the vibrational spacings of the S_1 and S_2 excited electronic states measured in Ne matrix with those derived from supersonic free jet data.[19(a)]

B. Neutral 1-methylphenanthrene

The absorption spectrum of neutral 1-methylphenanthrene has been studied in the ultraviolet and visible regions of the optical spectrum and the spectroscopy of this molecule is well documented, particularly for the solid phase at low temperature.[20(a)] This is, to the best of our knowledge, the first report of the ultraviolet to near-infrared absorption spectrum of 1-methylphenanthrene isolated in a rare gas (neon) matrix.

Substitution of a hydrogen at the position 1 with a methyl group [Fig. 6(b)] greatly reduces the symmetry of the molecular structure (from a C_{2v} to a C_1 symmetry representation group). The electronic states can no longer be represented by the C_{2v} group elements and so we simply label them S_i and T_i (i=0,1,...) for singlet and triplet electronic states, respectively. 1-methylphenanthrene has 14 π electrons which produce the low energy singlet–singlet and singlet–triplet transitions (type π–π^*) in the ultraviolet. Figure 2 shows the transitions from the ground (S_0) to the excited singlet states S_i (i=1,2,3,4,5,7) and to one of the excited triplet states (T_2).

By analogy with the assignment adopted for the transitions occurring in phenanthrene (see Sec. IV A), we assign the lowest energy absorption vibronic system observed in the spectrum of neutral 1-methylphenanthrene (Table II), to the singlet–triplet electronic transition, $T_2\leftarrow S_0$. All the other, higher energy transitions, are associated with the singlet manifold, and are assigned to the following transitions in order of increasing energy: $S_1\leftarrow X\ ^1A(S_0)$, $S_2\leftarrow X\ ^1A(S_0)$, $S_3\leftarrow X\ ^1A(S_0)$, $S_4\leftarrow X\ ^1A(S_0)$, $S_5\leftarrow X\ ^1A(S_0)$, $S_7\leftarrow X\ ^1A(S_0)$. [The $S_1\leftarrow X\ ^1A(S_0)$ and $S_2\leftarrow X\ ^1A(S_0)$ transitions correspond to the α and para bands in Clar's notation. In a similar manner, the $S_5\leftarrow X\ ^1A(S_0)$ and $S_7\leftarrow X\ ^1A(S_0)$ transitions are associated with the β and β' bands.]

A repeating pattern can be recognized in the energy intervals reported in Table II. These vibronic levels are compared with the vibrational intervals of phenanthrene in Table III and tentative vibrational assignments are proposed.

C. Phenanthrene cation

Assignments of the vibronic band systems produced by vacuum ultraviolet irradiation of phenanthrene isolated in a neon matrix which are associated with the molecular cation $C_{14}H_{10}^+$ are given in Table IV. These assignments are tentative in the absence of corroborative calculations of the cation's molecular orbitals (MO) which take into account the contribution of all the electrons of the system. A semiempirical approach is however possible using the Hückel molecular orbital (HMO) or PPP-SCF theories to calculate the energy of the π orbitals of the system.[10(c),12(b),22] The resulting π molecular orbital energy levels of phenanthrene are reported in Table V. The molecular orbitals are denoted following the symmetry of each species in the C_{2v} symmetry group representation. The observed cation absorption features—in order of increasing energy—[Figs. 3 and 5(a)] are, thus, assigned as follows:

(a) The very strong absorption system originating in the near infrared at 11 132 cm^{-1} (898.3 nm; see Table IV) is assigned to the $^2A_2(D_2)\leftarrow X\ ^2B_1(D_0)$ transition [calculated at 12 300,[10(c)] 12 340,[12(b)] and 10 501 (Ref. 22) cm^{-1}]. [The $^2A_2(D_1)\leftarrow X\ ^2B_1(D_0)$ transition into the first excited doublet state, $^2A_2(D_1)$, predicted by the HMO theory to fall in

TABLE IV. Vibronic transitions of phenanthrene and 1-methylphenanthrene cations isolated in a neon matrix. [Electronic transitions assigned following Ref. 12(b). The number in parentheses indicates the value of σ^2.]

Phenanthrene			1-Methylphenanthrene			Δ^c
λ (nm)	ν (cm^{-1})	$\Delta\nu$ (cm^{-1})	λ (nm)	ν (cm^{-1})	$\Delta\nu$ (cm^{-1})	$\Delta\nu$ (cm^{-1})
$^2B_1(D_7)\leftarrow X\ ^2B_1(D_0)$			$D_7\leftarrow X\ ^2A(D_0)$			
...	...	...	349.3 (0.1)	28 629	300	...
344.9 (0.5)	28 994	0	353.0 (0.1)[b]	28 329	0	665
$^2A_2(D_6)\leftarrow X\ ^2B_1(D_0)$			$D_6\leftarrow X\ ^2A(D_0)$			
389.9[a]	25 648	395	...	...	...	...
396.0 (0.3)[b]	25 252	0	404.5 (0.5)	24 655	0	597
$^2A_2(D_5)\leftarrow X\ ^2B_1(D_0)$			$D_5\leftarrow X\ ^2A(D_0)$			
408.1[a]	24 504	1 019 (2×507)	421.3 (0.5)	23 736	1 045	768
416.8[a]	23 992	507	433.0 (0.3)	23 095	404	897
425.8 (0.3)[b]	23 485	0	440.7 (0.3)[b]	22 691	0	794
$^2B_1(D_4)\leftarrow X\ ^2B_1(D_0)$			$D_4\leftarrow X\ ^2A(D_0)$			
460.3 (0.5)	21 725	480	467.1 (0.1)[b]	21 409	488	316
470.7 (0.2)[b]	21 245	0	478.0 (0.2)	20 921	0	324
$^2B_1(D_3)\leftarrow X\ ^2B_1(D_0)$						
634.4[a]	15 763	0	...	...	...	...
$^2A_2(D_2)\leftarrow X\ ^2B_1(D_0)$			$D_2\leftarrow X\ ^2A(D_0)$			
...	...	...	717.0 (0.3)	13 947	3 206 (2×1585)	...
748.5 (0.3)	13 360	2 228 (1406+818)	...	...	...	...
755.2 (0.3)	13 242	2 110 (1080+1042)	...	...	...	...
780.4 (0.3)	12 814	1 682 (1455+224)	802.8 (0.3)	12 456	1 715 (1385+308)	358
784.4 (0.3)	12 749	1 617 (2×818)	...	...	...	...
787.9 (0.2)	12 692	1 560 (1346+224)	811.3 (0.2)	12 326	1 585	366
794.5 (0.3)	12 587	1 455	820.4 (0.1)	12 189	1 448	398
797.6 (0.3)	12 538	1 406	...	...	...	...
801.4 (0.3)	12 478	1 346 (542+818)	824.7 (0.1)	12 126	1 385 (547+840)	352
818.9 (0.3)	12 211	1 080 (2×542)	...	...	...	...
821.4 (0.3)	12 174	1 042 (224+818)	...	...	...	...
823.5 (0.3)	12 143	1 011	...	...	...	...
836.8 (0.3)	11 950	818	863.5 (0.1)	11 581	840	369
856.6 (0.2)	11 674	542	885.9 (0.1)	11 288	547	386
880.6 (0.5)	11 356	224	905.1 (0.5)	11 049	308	307
898.3 (0.1)[b]	11 132	0	931.0 (0.1)[b]	10 741	0	391
908.2 (0.1)	11 011	(site)	...	...	...	...

[a]Represents a single measurement with a 0.5 nm uncertainty.
[b]Strongest band of the system.
[c]$\Delta\nu = \nu_{\text{Phenanthrene}} - \nu_{\text{Methylphenanthrene}}$.

the infrared at about 4430 cm^{-1}, is out of the range of the present study].

(b) The weak absorption band which appears at 15 763 cm^{-1} (634.4 nm) in a Ne matrix (not shown) is assigned to the $^2B_1(D_3)\leftarrow X\ ^2B_1(D_0)$ transition [calculated at 16 900,[10(c)] 16 370,[12(b)] and 15 155 (Ref. 22) cm^{-1}].

(c) The absorption at 21 245 cm^{-1} (470.7 nm) in Ne is assigned to the $^2B_1(D_4)\leftarrow X\ ^2B_1(D_0)$ transition [calculated at 19 900,[10(c)] 19 360,[12(b)] and 19 575 (Ref. 22) cm^{-1}].

(d) The absorption at 23 485 cm^{-1} (425.8 nm) in neon is assigned to the $^2A_2(D_5)\leftarrow X\ ^2B_1(D_0)$ transition (calculated at 22 400 [Ref. 10(c)] and 23 228 [Ref. 12(b)] cm^{-1}).

(e) The two high energy absorption bands observed in the near ultraviolet at 25 252 cm^{-1} (396.0 nm) and 28 994 cm^{-1} (344.9 nm) are assigned to the $^2A_2(D_6)\leftarrow X\ ^2B_1(D_0)$ transition {calculated at 26 300 [Ref. 10(c)] and 27 665 [Ref. 12(b)] cm^{-1}} and $^2B_1(D_7)\leftarrow X\ ^2B_1(D_0)$ transition {calculated at 29 761 [Ref. 12(b)] cm^{-1}}, respectively. {A higher energy transition, corresponding to the $^2B_1(D_8)\leftarrow X\ ^2B_1(D_0)$ transition and calculated at 316.3 nm,[10(c),12(b)] was not observed in neon. An absorption band associated with the phenanthrene cation has been reported, however, at 330.6±0.5 nm (Ref. 6) and 332 nm [Ref. 12(b)] in argon matrices at 4.2 and 20 K, respectively.}

Fundamental energy intervals (some of which exhibit a

TABLE V. Comparison of the phenanthrene cation optical transitions with the photoelectron spectra.

	I_i (eV)	I_i-I_1 (eV)	I_i-I_1 (nm)	I_i-I_1 (cm^{-1})	ν Ne (cm^{-1})	Assignment (electron promotion)
References 13(a)–13(c)					This work	
I_1	7.86	0		0		$X\ ^2B_1$
I_2	8.15	0.29	4 275.3	2 339	···	$^2A_2$ ($\pi^7\leftarrow\pi^6$)
I_3	9.28	1.42	873.1	11 453	11 132	$^2A_2$ ($\pi^7\leftarrow\pi^5$)
I_4	9.89	2.03	610.8	16 373	15 763	$^2B_1$ ($\pi^7\leftarrow\pi^4$)
I_5	10.59	2.73	454.2	22 019	21 245	$^2B_1$ ($\pi^7\leftarrow\pi^3$)
Reference 12(b)					This work	
I_1	7.87	0		0		$X\ ^2B_1$
I_2	8.15	0.28	4 428.7	2 258	···	$^2A_2$ ($\pi^7\leftarrow\pi^6$)
I_3	9.25	1.38	898.5	11 130	11 132	$^2A_2$ ($\pi^7\leftarrow\pi^5$)
I_4	9.85	1.98	626.2	15 970	15 763	$^2B_1$ ($\pi^7\leftarrow\pi^4$)
I_5	10.52	2.65	467.9	21 373	21 245	$^2B_1$ ($\pi^7\leftarrow\pi^3$)

repeating pattern) can be clearly recognized in the lowest energy absorption system of the cation at 224, 542, 818, 1011, 1042, 1346, 1406, 1455, 1560, and 1617 cm^{-1} in Ne at 4.2 K (Table IV). These vibrational frequencies are very close to the 545, 820, 1355, 1465, and 1555 values derived for the phenanthrene cation in solid argon at 20 K.[12(a)] Furthermore, the vibrational energies measured in neon for the ion D_2 state at 224, 542, 1042, 1346, and 1560 (Table IV) are also very close to the 210, 532, 1040, 1347, and 1540 cm^{-1} REMPI-PES values reported for the stronger vibrational transitions in the ground electronic state (D_0) of gas phase phenanthrene cation.[13(d)] This has two important implications. First, it indicates that the geometry of the phenanthrene cation is *similar* in the ground (D_0) and excited (D_2) electronic states. Second, it indicates that *the phenanthrene cation isolated in solid neon is not significantly perturbed by its environment* compared to the "ideal" case of the phenanthrene cation isolated in the gas phase. Thus, by analogy with the case of the neutral molecule (see Sec. III A and Table III), and noting that the geometry of the cation in its lower excited states is quite similar to that of the neutral molecule

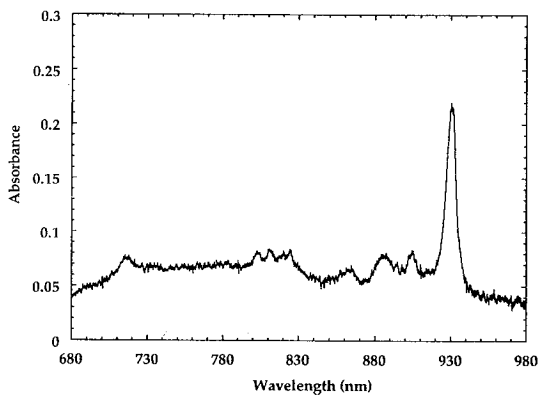

FIG. 4. The $D_2\leftarrow X\ ^2A(D_0)$ transition of the 1-methylphenanthrene cation isolated in a neon matrix (1-methylphenanthrene/neon=600, deposition rate=10 mmol h^{-1}, T=4.2 K). The spectrum corresponds to two, consecutive, 150 min deposits, each exposed to VUV irradiation for 30 min.

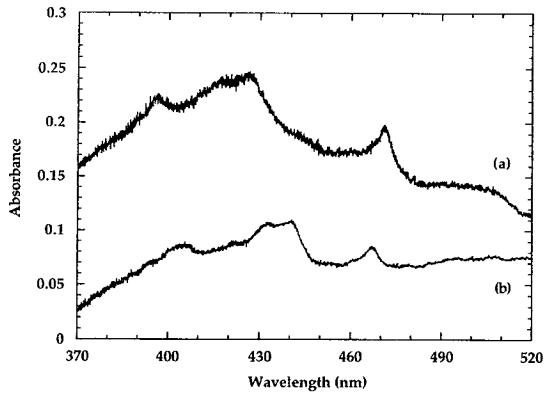

FIG. 5. The UV-to-visible absorption spectra of (a) the phenanthrene cation isolated in a neon matrix (phenanthrene/neon=1000, deposition rate=10 mmol h^{-1}, T=4.2 K). The spectrum corresponds to six, consecutive, 35 min deposits, each exposed to VUV irradiation for 16 min and (b) the 1-methylphenanthrene cation isolated in a neon matrix (phenanthrene/neon =600, deposition rate=10 mmol h^{-1}, T=4.2 K). The spectrum corresponds to two, consecutive, 150 min deposits, each exposed to VUV irradiation for 30 min.

(compare Tables I and IV), one can tentatively assign the cation vibrational intervals. Thus, we follow Andrews *et al.*,[12(a)] and assign the 1346, 1455, 1560, and 1617 cm^{-1} modes to C–C stretching modes (symmetric in-plane ring breathing of the conjugated ring systems[23]), the 542 mode to a symmetric deformation of the molecular ion, and the 818 cm^{-1} mode to the out-of-plane C–H bending mode. In the absence of detailed experimental and theoretical studies of the vibrational modes of $C_{14}H_{10}^+$ in the higher excited states it is unwarranted to speculate on their vibrational assignments.

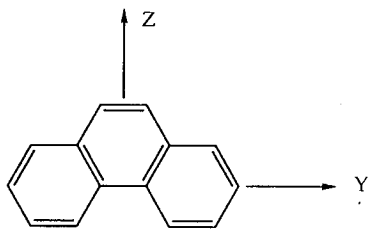

Phenanthrene

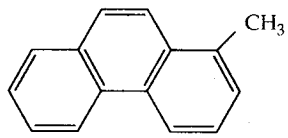

1-Methylphenanthrene

FIG. 6. The phenanthrene and 1-methylphenanthrene molecular representations and symmetry axes.

We note, however, that the 395 cm^{-1} vibrational interval of the $D_6 \leftarrow D_0$ transition is close to the 406 cm^{-1} symmetric deformation mode of phenanthrene.

D. 1-methylphenanthrene cation

Assignments of the vibronic band systems produced by vacuum ultraviolet irradiation of 1-methylphenanthrene isolated in a neon matrix which are associated with the molecular cation $(CH_3)C_{14}H_9^+$ are given in Table IV. These assignments are tentative in the absence of any other experimental and/or theoretical data on the 1-methylphenanthrene cation. Based on the strong similarity between the spectra of the phenanthrene and 1-methylphenanthrene cations isolated in neon (see Sec. III D) and the reduction in the symmetry representation of the molecular ion from (C_{2v}) for $C_{14}H_{10}^+$ to C_1 for $(CH_3)C_{14}H_9^+$, we assign the cation transitions as follows:

(a) The very strong absorption system originating in the near-infrared at 10 741 cm^{-1} (931.0 nm; see Table IV) is assigned to the $D_2 \leftarrow X\ ^2A(D_0)$ transition.

(b) The four following absorption bands observed at higher energies and peaking at 21 409 cm^{-1} (478.0 nm), 22 691 cm^{-1} (440.7 nm), 24 655 cm^{-1} (404.5 nm), and 28 329 cm^{-1} (353.0 nm), are assigned to the $D_i(i=4-7) \leftarrow X\ ^2A(D_0)$ transitions, respectively.

Six fundamental energy intervals (some of which exhibit a repeating pattern) can be clearly recognized in the lowest energy absorption system of the cation at 308, 547, 840, 1385, 1448, and 1585 cm^{-1} in Ne at 4.2 K. These vibrational frequencies are very close to the values observed for the phenanthrene cation (see Table IV and Sec. IV C). By analogy with the case of the neutral molecule (see Sec. III B), and considering that the geometry of the cation in its lower excited states should be quite similar to that of the neutral molecule, one can tentatively assign the cation vibrational intervals. Thus, we assign the 1385, 1448, and 1585 cm^{-1} modes to C–C stretching modes, the 547 mode to a symmetric deformation of the molecular ion, and the 840 cm^{-1} mode to the out-of-plane C–H bending mode. In the absence of any detailed experimental and theoretical studies of the vibrational modes of $(CH_3)C_{14}H_9^+$ it is unwarranted to speculate on their vibrational assignments. We note, however, that the 404 cm^{-1} vibrational interval of the $D_5 \leftarrow D_0$ transition is close to the 406 cm^{-1} symmetric deformation mode of phenanthrene.

E. Molar absorption coefficients

The molar absorption coefficients listed in Table VI for the phenanthrene cation in neon matrices were determined as follows. The number of neutral phenanthrene molecules depleted as a function of irradiation time was obtained from the relation $N = \Delta\tau/kf$. The absorbance, τ ($-\log_{10} I/I_0$), both before and after photolysis, was determined directly from the measured spectra (band integrated area), k is a constant ($\pi e^2/m_e c^2$) and the oscillator strength, f, was taken from Ref. 15. The 341.1 nm neutral phenanthrene band system ($S_1 \leftarrow S_0$) which has an f value of 2×10^{-4} was used to determine the number of neutral molecules depleted. System I was used as a reference point because it is the only unsaturated neutral band system remaining under the conditions required to yield satisfactory ion spectra (see Sec. III). In the calculations, it was assumed that for each neutral phenanthrene molecule depleted, a phenanthrene cation is formed. Note that while the absorption coefficients reported here are of the same order of magnitude as those previously reported for the matrix-isolated naphthalene cation,[4(a)] they are significantly lower (by a factor of 10^3–10^4) than those calculated by SCF-CI methods.[10(c),12(b),22] The same large discrepancy between measured and calculated f values has been reported for the naphthalene cation.[7] On the other hand, for the pyrene cation, a highly symmetrical PAH, the calculated[25] and neon matrix[5] values are much closer (0.36 and 0.13, respectively for the strongest transition at 439.5 nm). The observation of such large discrepancies may be due to the effect of the matrix cage on the oscillator strengths of charged species although this hypothetical effect seems difficult to reconcile with the low polarizability of the neon matrix. Another possibility is a fundamental flaw in the theoretical approach for the calculation of the oscillator strengths of charged molecular species. [Recent studies of the anthracene cation ($C_{14}H_{10}^+$) (Ref. 24) in the gas phase, using ion trap techniques, indicate a large discrepancy with the calculated oscillator strengths. The oscillator strengths derived from these experiments are of the same order of magnitude as those derived for the naphthalene[4(a)] and phenanthrene cations isolated in neon matrices.] This is an important problem which needs to be examined from the theoretical point of view.

TABLE VI. Phenanthrene cation vibronic transition oscillator strengths measured in a neon matrix are compared to the calculated values.

λ (nm)	ν (cm^{-1})	f_{Ne}^{a}	$f_{calculated}$
898.3	11 132	6.0 (−5)	1.0 (−1)[b]
			1.0 (−1)[c]
			1.6 (−1)[d]
856.6	11 674	0.9 (−5)	
470.7	21 245	5.1 (−5)	7.2 (−2)[b]
			6.5 (−2)[c]
			5.6 (−2)[d]
425.8	23 485	1.8 (−5)	1.1 (−1)[b]
			1.8 (−1)[c]
396.0	25 252	1.9 (−5)	1.3 (−1)[b]
			3.1 (−2)[c]
344.9	28 994	1.0 (−5)	6.0 (−3)[b]

[a]This work.
[b]Reference 12(b).
[c]Reference 10(c).
[d]Reference 22.

V. CONCLUSIONS

The ultraviolet-to-near infrared (180–1050 nm) absorption spectra of phenanthrene ($C_{14}H_{10}$), 1-methylphenanthrene [$(CH_3)C_{14}H_9$)] and their radical cations [$C_{14}H_{10}^+$ and $(CH_3)C_{14}H_9^+$], formed by direct vacuum-ultraviolet photoionization, have been studied in neon matrices. This study in solid Ne provides the first information on the spectroscopy of these molecular species *when (largely) unperturbed by the medium*, a condition which is crucial for astrophysical applications.

Nine ultraviolet absorption systems, having similar vibrational frequencies, are reported for the neutral molecules. The absorption spectrum of the phenanthrene radical cation isolated in solid Ne shows six progressions in the visible and the ultraviolet regions. Only five were detectable for its 1-methyl derivative. The measurements are in agreement with the photoelectron spectra of phenanthrene, the absorption spectra of phenanthrene cations in different media, and the predictions of semiempirical HMO and SCF-Cl calculations. Taken together, these similarities permit one to assign the electronic transitions of the cation. In the absence of any experimental and/or theoretical data on the 1-methylphenanthrene cation its observed vibronic transitions are assigned by analogy with the unsubstituted phenanthrene cation based on the striking similarity of the two spectra. The present results also stress the need for more sophisticated calculations to help resolve the important discrepancy between the f values measured for PAH radical cations isolated in neon matrices and their analogs derived from semiempirical calculations. These data, and similar studies on larger PAHs, are critically needed to interpret observations of the interstellar medium and have motivated the present program to provide a data base of the spectroscopy of neutral and ionized PAHs isolated in an inert medium.

ACKNOWLEDGMENTS

The authors want to thank R. Walker for his invaluable expert assistance in developing the experimental apparatus. The authors want also to express their gratitude to Professor T. Bally for communicating his unpublished experimental and theoretical results on $C_{14}H_{10}^+$. This project is supported by NASA Ultraviolet, Visible, and Gravitational Astrophysics Research and Analysis Program (Grant No. 188-41-57-41), NASA Long-Term Space Astrophysics Research Program (Grant No. 399-20-00-05) and NASA Infrared, Submillimiter, and Radio Astronomy Research and Analysis Program (Grant No. 188-44-57-01).

[1] (a) A. Léger and J. L. Puget, Astron. Astrophys. **137**, L5 (1984); (b) L. J. Allamandola, A. G. G. M. Tielens, and J. R. Barker, Astrophys. J. (Lett.) **290**, L25 (1985).

[2] (a) L. J. Allamandola, A. G. G. M. Tielens, and J. R. Barker, Astrophys. J. Suppl. Ser. **71**, 733 (1989); (b) J. L. Puget and A. Léger, Annu. Rev. Astron. Astrophys. **27**, 161 (1989).

[3] (a) G. P. Van der Zwet and L. J. Allamandola, Astron. Astrophys. **146**, 76 (1985); (b) A. Léger and L. B. d'Hendecourt, *ibid.*, **81** (1985); (c) M. K. Crawford, A. G. G. M. Tielens, and L. J. Allamandola, Astrophys. J. (Lett.) **293**, L45 (1985); (d) G. H. Herbig and K. D. Leka, Astrophys. J. **382**, 193 (1991); (e) P. Jenniskens and X. Désert, Astron. Astrophys. Suppl. Ser. **106**, 39 (1994); (f) C. Joblin, J. P. Maillard, L. d'Hendecourt, and A. Léger, Nature **346**, 729 (1990).

[4] (a) F. Salama and L. J. Allamandola, J. Chem. Phys. **94**, 6964 (1991); (b) **95**, 6190 (1991); (c) Astrophys. J. **395**, 301 (1992).

[5] F. Salama and L. J. Allamandola, Nature **358**, 42 (1992).

[6] F. Salama and L. J. Allamandola, J. Chem. Soc. Faraday Trans. **89**, 2277 (1993).

[7] P. Du, F. Salama, and G. H. Loew, Chem. Phys. **173**, 421 (1993).

[8] (a) B. Meyer, *Low Temperature Spectroscopy* (Elsevier, New York, 1971); H. E. Hallam, in *Vibrational Spectroscopy of Trapped Species*, edited by H. E. Hallam (Wiley, New York, 1973), p. 11.

[9] (a) V. E. Bondybey and T. A. Miller, in *Molecular ions: Spectroscopy, Structure and Chemistry*, edited by T. A. Miller and V. E. Bondybey (North--Holland, New York, 1983), p. 125; (b) H. Jodl, in *Chemistry and Physics of Matrix-Isolated Species*, edited by L. Andrews and M. Moskovits (North–Holland, New York, 1989), p. 343.

[10] (a) T. Shida and W. H. Hamill, J. Chem. Phys. **44**, 2375 (1966); (b) T. Shida and S. Iwata, J. Am. Chem. Soc. **95**, 3473 (1973); (c) Z. H. Khan, Acta Phys. Pol. A **82**, 937 (1992).

[11] O. Brede, W. Helmstreit, and R. Mehnert, Chem. Phys. Lett. **28**, 43 (1974).

[12] (a) L. Andrews, R. S. Friedman, and B. J. Kelsall, J. Phys. Chem. **89**, 4016 (1985); (b) T. Bally (private communication, 1993).

[13] (a) S. Obenland and W. Schmidt, J. Am. Chem. Soc. **97**, 6633 (1975); (b) E. Clar and W. Schmidt, Tetrahedron **32**, 2563 (1976); (c) W. Schmidt, J. Chem. Phys. **66**, 828 (1977); (d) N. Thantu and P. M. Weber, Z. Phys. D **28**, 191 (1993).

[14] C. M. White, J. Chem. Eng. Data **31**, 198 (1986).

[15] P. Swiderek, M. Michaud, G. Hohlneicher, and L. Sanche, Chem. Phys. Lett. **178**, 289 (1991).

[16] S. J. Cyvin, G. Neerland, J. Brunvoll, and B. N. Cyvin, Spectrosc. Lett. **14**, 37 (1981).

[17] M. L. Klein and J. A. Venables, in *Rare Gas Solids* (Academic, London, 1976), Vol. 1.

[18] L. Andrews, B. J. Kelsall, and T. A. Blankenship, J. Phys. Chem. **86**, 2917 (1982).

[19] (a) N. Ohta and H. Baba, Mol. Phys. **59**, 921 (1986); (b) W. Karcher, R. J. Fordham, J. J. Dubois, P. G. J. M. Glaude, and J. A. M. Ligthart, in *Spectral Atlas of Polycyclic Aromatic Compounds*, edited by the Commission of the European Communities (Reidel, Dordrecht, 1983), p. 52.

[20] (a) I. A. Nakhimovsky, M. Lamotte, and J. Joussot-Dubien, in *Handbook of low temperature electronic spectra of polycyclic aromatic hydrocarbons* (Elsevier, Amsterdam, 1989), p. 211; (b) V. Schettino, N. Neto, and S. Califano, J. Chem. Phys. **44**, 2724 (1966).

[21] S. Grimme and H. G. Lohmannnsroben, J. Phys. Chem. **96**, 7005 (1982).

[22] O. Parisel, G. Berthier, and Y. Ellinger, Astron. Astrophys. **266**, L1 (1992).

[23] R. Rumelfanger, S. A. Asher, and M. B. Perry, Appl. Spectrosc. **42**, 267 (1988).

[24] P. Boissel, in *The Diffuse Interstellar Bands*, edited by A. G. G. M. Tielens and T. Snow (Kluwer Academic, New York, in press).

[25] M. Vala, J. Szczepanski, F. Pauzat, O. Parisel, D. Talbi, and Y. Ellinger, J. Phys. Chem. (in press).